Cloudstreets *Theory and Satellite Observations*

By Dr. Joachim P. Kuettner, Marshall Space Flight Center, National Aeronautics and Space Administration, Huntsville, Alabama, USA

Presented at the 10th OSTIV Congress, South Cerney (England), June 1965

A. Observations

In Part 1 (Kuettner, 1959), the band structure of the atmosphere was studied by ground and aircraft observations. For convective cloudstreets near the ground, over the ocean, in squall lines, hurricanes and jetstreams, the existence of a typical wind profile was established. This profile is strongly curved with little directional change with height. Frequently a wind maximum exists within the convective layer and an inversion on top of it. A characteristic value of the curvature is 10^{-7} cm^{-1} sec^{-1}. The spacing (center to center) between these cloudstreets which are oriented along the wind direction generally lies between 2 and 3 times the height.

Since 1960, weather satellites have confirmed the widespread existence of atmospheric cloudbands on different scales. In this investigation, attention is focused again on the convective scale. Tiros and Nimbus pictures from oceans, continents (arctic to tropical) show individual or multiple cloudstreets of considerable length, sometimes exceeding 400 miles. In those cases where aerological data are available from the place and time of the satellite observations, the curved wind profile was again present. In view of the similarity of cloudstreets and mountain waves as seen from satellite altitude, the orientation of the cloudbands to the wind direction has to be used as a clue.

In the following, a theory of organized convection is developed based on an extension of the cellular convection theory for a medium with arbitrary but unidirectional flow profile.

B. Theory

1. General Description of Mechanism

The findings of the aerological study related in Part 1 (Kuettner, 1959) suggest that vorticity forces enter the convective mechanism. The restoring forces experienced by a displaced parcel conserving its vorticity in an environment of differant vorticity tend to return the parcel to its original level. This mechanism also underlies the Rossby Waves in the Westerlies and the Tollmien-Schlichting waves in the boundary layer.

In our case, the curved vertical wind profile (shear gradient) found under cloud street conditions represents the vorticity gradient and the resulting restoring forces counteract the convective motions. This situation resembles that of a stable temperature stratification.

There is, however, one particular mode of convection which eliminates this stability. If the convective elements are two-dimensional such that all circulations take place in planes *normal* to the flow direction ("longitudinal rolls", fig. 1) no restoring forces arise since no vorticity gradient exists in these planes. On the other side, in planes parallel to the flow, the fluid parcels rise and fall jointly and have no differential vorticity. Therefore, they do not experience restoring forces.

By introducing the vorticity gradient into the equations of the classical theory of cellular convection (Rayleigh, 1916) the results of this theory are modified as follows:

The critical Rayleigh number which characterizes the onset of convection in a medium at rest holds, in the presence of a curved velocity profile, only for longitudinal rolls. All other convection modes, e. g., three-dimensional cells (fig. 2) require higher Rayleigh numbers, i. e., higher vertical density gradients.

In the atmosphere, the observed vertical wind shear gradients create stabilizing forces which are of the same order of magnitude as the buoyancy forces. Therefore, as solar-heating of the ground proceeds in the morning, three-dimensional convection cells may still be entirely suppressed while two-dimensional cells stretching in the wind direction are already highly amplified. Later, three-dimensional convection may also amplify but the Rayleigh numbers of the two modes will remain different by as much as several orders of magnitude. Thus longitudinal bands represent the convection mode which will prevail during the day.

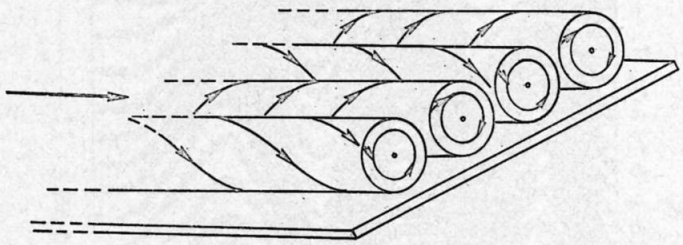

Fig. 1

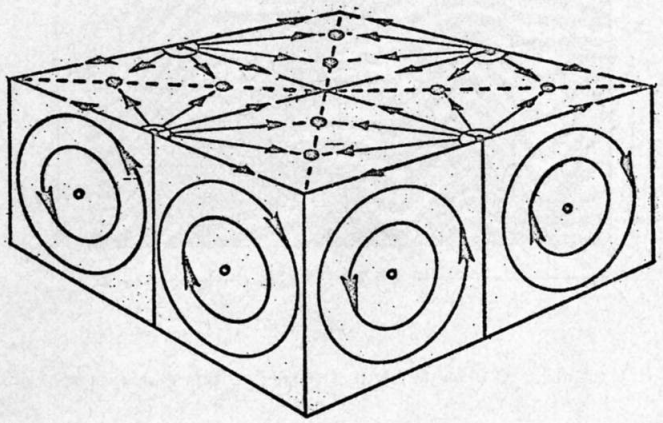

Fig. 2

2. Theory of Convection Bands

The following simplified flow conditions are assumed: An incompressible, viscous and conductive fluid of height H and of infinite horizontal extension flows steadily and under gravity over flat ground in the horizontal x direction. Its speed (but not its direction) varies with height. (See fig. 3.)

The vertical density gradient is constant and positive, setting the stage for convection. It shall be small compared to the density itself. Therefore, their ratio will be neglected everywhere except in its "buoyancy" function, i. e., in connection with gravity. (Boussinesq's principle; first applied to the problem of cellular convection by Rayleigh, 1916.)

It is furthermore assumed that the kinematic viscosity ν and the heat diffusivity k are invariant throughout the medium[1] and that a linear thermal expansion function holds for the small density changes under consideration. Also, the lifetime of the convective circulations shall be small enough to remain unaffected by the earth's rotation (order of magnitude of one hour).

Using "small perturbation" methods, all products of small quantities will be neglected. The properties of the basic flow to be designated by symbols with a bar ($^-$) shall be functions of height only except the pressure which shall fall off in the flow direction to keep the flow steady against viscosity. Perturbation quantities will be expressed by the same symbols as the basic quantities but without a bar. Prime, ( )' and double prime, ( )" denote first and second derivatives with respect to height.

Using a ground fixed conventional Cartesian coordinate system, x and y being the horizontal coordinates, u and v the corresponding horizontal velocity components, z the vertical coordinate and w the vertical velocity component, the foremented assumptions can be expressed in the following way:

$$\left.\begin{array}{l} \partial/\partial t,\ \partial/\partial y\,(\bar{\varrho}, \bar{P}, \bar{u}) = \partial/\partial x\,(\bar{\varrho}, \bar{u}) = \bar{v} = \bar{w} = 0 \\ \bar{\varrho}',\ \partial\varrho/\partial T,\ \nu,\ K = \text{constant} \end{array}\right\} \quad (1)$$

Here, ρ = density, P = pressure, T = temperature, τ = time, ν = kinematic viscosity and K = heat diffusivity.

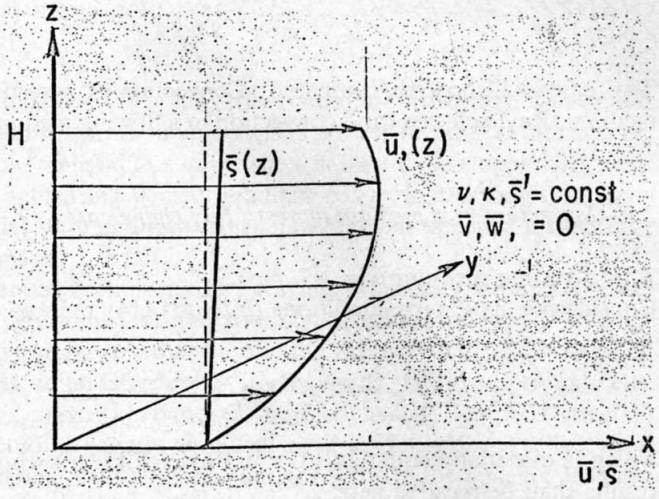

Fig. 3

[1] Later an exception to this assumption will be discussed.

Under these conditions, the following Navier-Stokes perturbation[2] equations hold:

$$f(u) + \bar{u}'w - \varrho\nu\bar{u}''/\bar{\varrho} = -(1/\bar{\varrho})\,\partial p/\partial x \quad (2a)$$

$$f(v) = -(1/\bar{\varrho})\,\partial p/\partial y \quad (2b)$$

$$f(w) + g\varrho/\bar{\varrho} = -(1/\bar{\varrho})\,\partial p/\partial z \quad (2c)$$

where g = gravity.

The function f is defined as

$$f \equiv \partial/\partial t + \bar{u}\,\partial/\partial x - \nu\nabla^2 \quad (2d)$$

where ∇^2 is the three dimensional Laplacean operator.

$$\nabla^2 = \partial^2/\partial x^2 + \partial^2/\partial y^2 + \partial^2/\partial z^2$$

The continuity equation for incompressible flow requires that the divergence

$$(\partial u/\partial x + \partial v/\partial y + w') = 0 \quad (3)$$

The energy equation is given by

$$F(T) + \bar{T}'w = 0 \quad (4a)$$

Here the function F is defined by

$$F \equiv \partial/\partial t + \bar{u}\,\partial/\partial x - K\nabla^2 \quad (4b)$$

Making use of the linear thermal expansion function listed under (1), we may prefer to express relation (4a) directly in terms of the density ρ

$$F(\varrho) + \bar{\varrho}'w = 0 \quad (4c)$$

Cross differentiating (2a), (2b), and (2c) the perturbation velocities u and v may be eliminated by way of (3), yielding

$$2\bar{u}'\partial w/\partial x + (1/\bar{\varrho})\left[g\varrho' - \nu\bar{u}''\partial\varrho/\partial x\right] = -(1/\bar{\varrho})\nabla^2 p$$

Assuming that ρ' and $\partial\rho/\partial\chi$ are of comparable magnitude[3] the second term in the bracket can be neglected against the first one, since the earth's gravity g is at least 2 or 3 orders of magnitude larger than the quantity $\nu\,\bar{u}''$ encountered in the atmosphere[4]. This reduces the above equation to

$$2\bar{u}'\partial w/\partial x + g\varrho'/\bar{\varrho} = -(1/\bar{\varrho})\nabla^2 p \quad (5)$$

---

[2] The basic flow equations have been subtracted from the full Navier-Stokes equations.

[3] This is later borne out in the cellular solution, the ratio of ρ' to $\partial\rho/\partial x$ being a measure of the vertical and horizontal dimensions of the convective elements.

[4] For vertical motions, atmospheric eddy viscosity

$\nu \leqq 10^7\ cm^2\,sec^{-1}$ even in strong turbulence, and the vertical gradient of the wind shears of the basic flow

$|\bar{u}''| \leqq 10^{-6}\ cm^{-1}\,sec^{-1}$, even under jetstream conditions (See Part I therefore).

$g/\nu\bar{u}'' \geqslant 10^2$.

which allows us to eliminate the perturbation pressure P between (2c) and (5) by cross differentiation.

Making use again of Boussinesq's principle, we obtain

$$f\left(\nabla^2 w\right) - \bar{u}''\,\partial w/\partial x + g\,\nabla_h^2 \varrho/\bar{\varrho} = 0 \tag{6}$$

where ∇_h^2 is now the two dimensional Laplacean operator applied in the horizontal plane only:

$$\nabla_h^2 = \partial^2/\partial x^2 + \partial^2/\partial y^2 \tag{6a}$$

We are now left with equations (4c) and (6) connecting vertical velocity ω and density ρ of the perturbation field. Eliminating the variable ρ between these equations by cross application of the operators ∇_h^2 and F and introducing the instability parameter

$$\beta = \bar{\varrho}'/\bar{\varrho} \tag{6b}$$

we arrive at a 6th order differential equation for the vertical velocity component w which may be considered the basic equation of our problem:

$$\left\{ F\left[f\left(\nabla^2\right) - \bar{u}''\,\partial/\partial x\right] - g\beta\,\nabla_h^2 \right\} w = 0 \tag{7}$$

It the flow is steady ($\partial/\partial\tau = 0$), inviscous ($\nu = 0$), nonconductive ($K = 0$) and two dimensional ($\partial^2/\partial y^2 = 0$), the operator $f = F = \bar{u}\,\partial/\partial x$, see (2d) and 4b), and equation (7) reduces to

$$\partial^2 w/\partial x^2 + w'' - \left(g\beta/\bar{u}^2 + \bar{u}''/\bar{u}\right) w = 0 \tag{8}$$

which is the well known wave equation governing for example the airflow over mountains (lee wave problem[5]).

Treatment of the complete equation (7) shall be facilitated by the following simplifications.

In analogy to certain boundary layer studies, the height dependent flow velocity $\bar{u}(z)$ will be approximated by a mean velocity $\bar{\bar{u}}$ of the layer under consideration. (Regarding the unidirectional character of the flow, see the atmospheric observations presented in Part I.)

Likewise, the curvature $\bar{u}''$ of the vertical wind profile shall be expressed by a characteristic mean value $\overline{\bar{u}''}$. It may be recalled here from Part I that the investigation of cloud-streets in the atmosphere reveals a uniform curvature with a typical value

$$\overline{\bar{u}''} = 10^{-7}\left(cm^{-1}\,sec^{-1}\right)$$

Introducing three dimensional harmonic perturbations, we need to leave the door open for exponential amplification or damping. If l and m are wave numbers along x and y, such that

$$l = 2\pi/\lambda_x;\quad m = 2\pi/\lambda_y, \tag{9}$$

λx and λy denoting the wavelengths in the x and y direction respectively, and if σ is the exponential time constant (a complex quantity), all perturbations will contain the factor

$$\exp\left[i\left(lx + my\right) + \sigma t\right]$$

where

$$\sigma = \sigma_r + i\sigma_i$$

With all basic quantities in (7) now invariant, harmonic variations of w with height are admissable, the phase of which depends on the boundary conditions.

Rayleigh (1916) in his classical theory of cellular convection selected those boundary conditions "which are simplest from the mathematical point of view", namely, free surfaces at the top and bottom:

$$w = w'' = 0 \quad at\ z = 0, H. \tag{10}$$

More realistic boundary conditions were later investigated by Jeffreys (*1926*) and Pellew and Southwell (*1940*) without affecting the validity of Rayleigh's basic conclusions.

By retaining Rayleigh's boundary conditions, the fundamental difference of convection in a resting and in a moving medium can be demonstrated in the simplest fashion. We will therefore apply (10) in our study.

Assuming w proportional to *sin nz*, the above boundary conditions are satisfied by

$$n = \gamma\pi/H \tag{11}$$

where γ an integer. With

$$w'' = -n^2 w$$

the operators used earlier reduce to

$$\left.\begin{aligned} \nabla^2 &= -\left(l^2 + m^2 + n^2\right) \\ \nabla_h^2 &= -\left(l^2 + m^2\right) \\ f &= \sigma_r + \nu d^2 + iS \\ F &= \sigma_r + K d^2 + iS \end{aligned}\right\} \tag{12}$$

Here

$$S = \left(\sigma_i + \bar{\bar{u}} l\right) \tag{12a}$$

For simplicity, we introduce furthermore the following quantity

$$d^2 = l^2 + m^2 + n^2 \tag{13}$$

Dividing (7) by w and introducing (12), (12a) and (13)

$$\left(\sigma_r + K d^2 + iS\right)\left[\left(\sigma_r + \nu d^2 + iS\right) d^2 + il\bar{u}''\right] - g\beta\left(l^2 + m^2\right) = 0 \tag{14}$$

Two cases will now be compared: Convection in a resting medium (Rayleigh case) and convection in a flowing medium.

2.1. *Convection in a medium at rest (Rayleigh's case)*

In a resting medium $\bar{\bar{u}} = \overline{\bar{u}''} = 0$

Considering stationary conditions ($\sigma_1 = 0$) (14) reduces to

$$\left(\sigma_r + K d^2\right)\left(\sigma_r + \nu d^2\right) d^2 - g\beta\left(l^2 + m^2\right) = 0 \tag{15}$$

which is essentially equation (37) of Rayleigh (1916) whose results shall be recalled here.

Obviously σ_r, the real part of the amplification σ, is a function of the cell size and reaches a maximum for a certain combination of the horizontal cell dimensions expressed by

---

[5] Regarding compressible flow, see, for example, Alaka, Queney, et al, 1960, equation (39a).

l and m in relation to the vertical dimension expressed by n. Rayleigh considers the case of "marginal stability" where the maximum amplification

$$\sigma_{max} = 0 \tag{16}$$

Here the density gradient β is just large enough to permit the onset of convection. This assumption permits Rayleigh to derive the optimum cell dimensions in the simplest conceivable way by differentiation of σ_r with respect to d^2 resulting in the relation

$$d^2 = (3/2)n^2 \tag{17}$$

see Rayleigh's (1916) equation (42). This in turn requires a vertical density gradient

$$\beta = 27 \kappa\nu n^4/4g$$

Evidently the minimum value of β is given by the minimum value of n, i. e., by $\gamma = 1$, see (11). Therefore

$$n = \pi/H \tag{18}$$

which results in the well-known critical *Rayleigh number* for "marginal stability"

$$R_{cr} = g\beta H^4/\kappa\nu = 27\pi^4/4 \sim 658 \tag{19}$$

Hence the required density gradient

$$\beta_{cr} = 27\pi^4 \nu\kappa/4gH^4 \tag{20}$$

The corresponding values of R_{cr} for more realistic boundary conditions (both boundaries fixed or one free, one fixed, see Jeffreys (1926); Pellew and Southwell (1940) range from 1100 to 1700.

For symetrical cells (l = m) the horizontal wavelength λ is 4 times the height of the convective layer, see (17) in connection with (9) and (18),

$$\lambda = 4H \tag{21}$$

Figure 2 illustrates this case.

If the stability is not marginal and the density gradient is large enough to create a finite amplification ($\sigma_{max} > 0$), equation (15) which is cubic in d^2 leads to the condition

$$(l^2 + m^2) > n^2/2$$

instead of (17), i. e., the optimum horizontal dimensions begin to shrink in comparison with their vertical dimensions. How realistic this conclusion is may be left open here since an increasing density gradient passes first through the marginal state and its further development depends on the heat transfer.

It has been noticed by Rayleigh that only the sum (l^2+m^2) is determined by the stability criterion, but not l^2 and m^2 separately. In other words, the ratio of the (horizontal) cell sides is undetermined. For example, two-dimensional cells, i. e., convection bands (also called "rolls", "strips", "streets") would be equally amplified as three-dimensional cells ("symmetrical cells"[6]) such that for l = 0 the spacing between bands would not be given by (21) but by

$$\lambda = 2\sqrt{2}\, H \tag{22}$$

Figure 1 illustrates this case. Rayleigh states this undeterminedness as follows: "I do not see that any plausible hypothesis as to the origin of the initial disturbances leads us to expect one particular ratio of sides in preference to another."

This situation changes if convection takes place in a flowing medium.

2.2. *Convection in a flowing medium*

To solve the more general equation (14) with $\bar{u}, \overline{u''} \neq 0$ we may, in a first approximation, neglect the difference between the diffusivities for momentum and for heat. In other words, we assume the Prandtl numbers to be unity

$$P_r = \nu/\kappa = 1 \tag{23}$$

Since the parameters f and F are now identical, we introduce the quantity

$$\gamma = fd^2 = Fd^2 = (\sigma_r + \nu^* d^2 + is)d^2 \tag{24}$$

Here

$$\nu^* = (\kappa\nu)^{1/2} \tag{25}$$

This may serve to remember that both heat conductivity and viscosity have been taken into account here, but that they are assumed to be numerically equal.

Introducing (24) into (14) the following quadratic equation results

$$\gamma^2 + il\overline{u''}\gamma - g\beta(l^2+m^2)d^2 = 0 \tag{26}$$

The amplification constant is now given by

$$\sigma_r = \mp\left[g\beta(l^2+m^2)/d^2 - (l\overline{u''}/2d^2)^2\right]^{1/2} - \nu^* d^2 \tag{27}$$

which is the real part of the solution of (26). This relation between amplification and cell size in non-uniform flow was already cited in Part I and shall now be discussed.

The choice of sign in front of the bracket indicates the possibility of a positive growth rate.

The first term in the bracket containing gravity and density gradient represents the buoyancy. A negative density gradient yielding an imaginary σ will produce gravity waves, see also (8). The magnitude of the buoyancy term depends on the cell dimensions such that, with decreasing horizontal cell size (increasing l and m) it tends towards a finite maximum value $g\beta$.

The second expression in the bracket is the vorticity term. Regardless of the sign of the shear gradient $\overline{u''}$ (which appears in the squared form only) this term always subtracts from the buoyancy. In the absence of buoyancy, the vorticity term is responsible for the type of waves, which appear as Tollmien-Schlichting waves in the boundary layer or as Rossby waves in the planetary westerlies. Such inertia waves owe their restoring force to the conservation of vorticity in displaced parcels which move in a field of nonconstant vorticity (Lin, 1955).

---

[6] Symmetrical with respect to their vertical axis.

The last term of (27), the viscosity/conductivity term, is always negative and tends to suppress or dampen buoyant motions.

This brings us to the general behavior of the growth rate ρ_r in (27) as a function of the horizontal wave numbers l and m. A three dimensional presentation of this function is given in figure 4.

2.2.1. General behavior of growth rate as a function of wavelength.

Figure 4 illustrates the function σ_r (l, m) for positive and negative wavenumbers (although, for the purpose of this study, we are interested only in positive l and m). The "jelly-fishlike" body in figure 4 has the following characteristics:

It its center, that is at m = l = 0, σ_r has a minimum and is negative. (From now on, σ_r will be replaced by σ, with the understanding that we are talking about a real quantity.) Since l and m are wave numbers, their reciprocal quantities, the wavelengths, tend at this point towards infinity and correspond to one unlimited symetric convective cell. Due to viscosity/conductivity and vanishing buoyancy, the motion dies out. At the other end, as l and m grow without limit (the cells getting narrower and narrower) σ tends toward minus infinity. Here the motion dies out likewise, due to rapidly increasing conductivity and viscosity forces.

Between two extremes, there is a range of cell dimensions where Z reaches a maximum which may be positive depending on the magnitude of β in the buoyancy term.

If the medium is *at rest* (Rayleigh case, discussed above), the maximum of σ is characterized by a circular ridge of constant elevation (dashed circle through A and A'). The radial nature of this ridge indicates that maximum amplification applies to any combination of l and m resulting in a certain critical value of (l^2+m^2). This illustrates that there is no preference for a definite ration of the cell sides (Rayleigh's "Undeterminedness Theorem").

If the medium is *flowing* in the x direction with a vertical flow profile of curvature $\overline{\overline{u}}$" the circular ridge of maximum amplification is deformed. Slopes develop toward the l axis such that saddle points form there and peaks over the m axis. Compared to the circular ridge of a resting medium, position and elevation of the maxima over the m axis remain uns changed while those over the l axis are displaced and depresed.

The local maxima over the m axis imply that the emerging cell form is now uniquely determined by the condition l = 0, i. e., two dimensional convection bands stretching without limit in the direction of flow. This illustrates that Rayleigh's "Undeterminedness Theorem" is removed for the case of a flowing medium.

The growth rate illustrated in figure 4 will now be derived from equation. (27)

2.2.2. Convection Pattern in a Flowing Medium

Introducing the quantity

$$\varphi = \left[g\beta\left(1-n^2/d^2\right) - \left(\ell\overline{\overline{u}}''/2d^2\right)^2\right]^{1/2} \tag{28}$$

equation (27) may be rewritten as

$$\sigma = \mp\varphi - \nu^* d^2 \tag{29}$$

Cell dimensions l and m yielding maximum growth rate σ, as determined by

$$\partial\sigma/\partial\ell = \partial\sigma/\partial m = 0$$

are given by

$$\left[\left(\psi - \overline{\overline{u}}''^2/4\right)/\varphi d^4 - 2\nu^*\right]\ell = 0 \tag{30}$$

and

$$\left\{\left(\psi/\varphi d^4\right) - 2\nu^*\right\} m = 0 \tag{31}$$

Here

$$\psi = g\beta n^2 + \ell^2\overline{\overline{u}}''^2/2d^2 \tag{32}$$

The following alternatives result:

$$\ell = m = 0 \tag{33}$$

$$\ell = 0;\ \left\{\left(\psi/\varphi d^4\right) - 2\nu^*\right\} = 0 \tag{34}$$

$$m = 0;\ \left[\left(\psi - \overline{\overline{u}}''^2/4\right)/\varphi d^4 - 2\nu^*\right] = 0 \tag{35}$$

The remaining alternative requires infinite d^2 corresponding to zero-width of the cells and results in $\sigma = -\infty$, due to viscosity and conductivity (see fig. 4). It is without interest to us.

Obviously, the first alternative (33), represents the finite minimum in the center of figure 4, corresponding to a convection cell of infinite horizontal extension.

Here

$$\sigma = -\nu^* d^2$$

and the motion is damped.

Case (34) represents the maximum elevation of σ over the m axis and corresponds to bands *along* the flow direction ($\lambda x = \infty$). Case (35) represents the saddle points over the l axis and represents bands *across* the flow direction ($\lambda y = \infty$).

It remains to be shown that the condition l = 0 describes indeed the absolute maximum as far as the growth rate is concerned.

Fig. 4

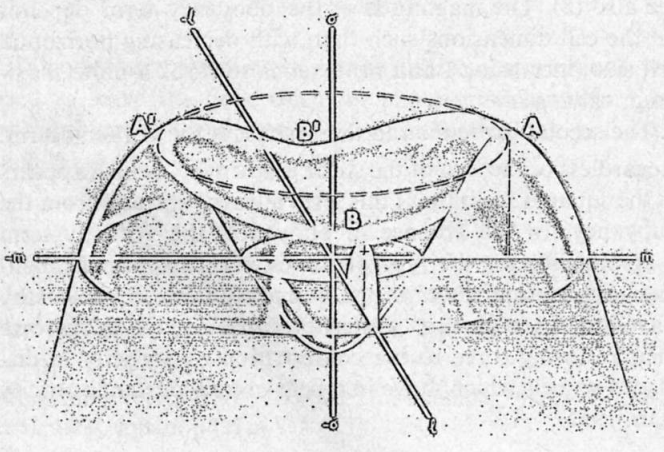

Taking advantage of the "marginal stability" assumption of Rayleigh, see (16), this can be done in the following way.

First, it will be shown that case (34) results in the same critical Rayleigh number as that derived for a resting medium, while case (35) requires a higher Rayleigh number and therefore a larger vertical density gradient β. In other words, for a given β, case (34) yields a higher growth rate than case (35).

Subsequently, it will be confirmed, by second derivatives, that (35), in contrast to (34), describes indeed a saddle point.

Case 1: Bands Along Flow Direction

Taking alternative (34) first and introducing it into (29), again under the condition of marginal stability given by (16), we obtain

$$\psi = 2\varphi^2 d^2$$

Substituting (28) and (32), with l = 0 and m = 0, the cell dimensions are determined by the relation

$$d^2 = (3/2)\, n^2 \tag{36}$$

This is identical with Rayleigh's case for a medium at rest, see (17). Introduction of (36) into (29), for $\sigma = 0$, yields again the Rayleigh number given by (19) and the critical density gradient given by (20).

Now however, Rayleigh's undeterminedness regarding the ratio of cell sides is removed. There is no question anymore whether (21) or (22) applies. With l = 0, the convection cells are bands along the flow direction and their approximate spacing as given by (22) is

$$\lambda_y \sim 2.8\, H \tag{37}$$

under the assumed boundary conditions. Figure 1 illustrates this case.

Case 2: Bands Across the Flow Direction

We now turn to the other alternative, (35), and introduce it into (29), again implying "marginal stability". We now obtain

$$\psi - \bar{u}''^2/4 = 2\varphi^2 d^2$$

Substituting (28) and (32), where m = 0 and l ≠ 0

$$d^2 = (3/2)\, n^2 \left[1 - \left(\bar{u}''^2 / g\beta n^2 \right) \left(1/4 - n^2/3d^2 \right) \right] \tag{38}$$

The quantity $\bar{u}''^2/g\beta n^2$ relates inertia to buoyancy forces and may be considered the *Froude number* ε of the model. It is responsible for the changes in the cellular pattern from a medium at rest.

Assuming, in a first approximation, that the Froude number is small in comparison with unity, i. e.,

$$\varepsilon = \bar{u}''^2/g\beta n^2 \ll 1 \tag{39}$$

we may neglect products of small quantities. (38) then results in

$$d^2 = (3/2)\, n^2 (1 - \varepsilon/36) \tag{40}$$

which should be compared to (36). Introducing (40) into (29) in connection with (16) the critical Rayleigh number now is

$$R_{cr} = (27\pi^4/4)(1 + \varepsilon/4) \tag{41}$$

in contrast to (19). This implies that the minimum density gradient producing positive growth rate has to be larger than in the previous case, namely

$$\beta = (27\pi^4 \nu\kappa / 4g H^4)(1 + \varepsilon/4) \tag{42}$$

This should be compared to (20) which is applicable to Case l.

Thus, a density gradient sufficient to produce convective bands oriented along the flow direction will not suffice to produce bands across the flow direction. "Longitudinal rolls", as postulated by alternative (34) emerge as the prevailing convection pattern in a flowing medium.

A cursory check of the magnitude of ε in the atmosphere, see Part I, suggests that it is considerably larger than unity and that (39) does not hold in the atmosphere. This implies that the Froude number effect is actually stronger than indicated in this simplified treatment.

Therefore convection bands in the flow direction are highly favored in the atmosphere in comparison to all other modes.

Finally, it shall be confirmed that Case 2 (alternative 35) describes indeed a saddle point, see point B over the l-axis in figure 4, while Case 1 (alternative 34) describes a local maximum, see point A over the m-axis.

Again we utilize the condition of marginal stability (16). Differentiating (30) with respect to l and (31) with respect to m and applying (34) and (35) respectively,

$$\left(\partial^2 \psi / \partial l^2 \right)_{l=0} = - \bar{u}''^2 / 4\varphi d^4$$

and

$$\left(\partial^2 \psi / \partial m^2 \right)_{m=0} = + \bar{u}''^2 / 4\varphi d^4$$

which confirms our conclusion.

Application to the Atmosphere

In applying the foregoing theory to the atmosphere, certain adjustments and a review of the simplifying assumptions are necessary.

The adiabatic behavior of the atmosphere as a gas requires that the stability parameter β, see (6b), be expressed in the well-known fashion bv the potential temperature θ such that

$$\beta = -\theta'/\theta \tag{43}$$

The assumption that the Prandtl number be unity, see (23), appears fairly compatible with the observations of eddy viscosity and conductivity in an atmosphere near neutral stability (Lumley and Panofsky, 1964) whereas such value would be unpermissible for most liquids.

As far as Rayleigh's simplified boundary conditions (2 free surfaces) are concerned, it has been shown by Jeffreys (1926) and by Pellew and Southwell (1940) that more realistic boundary conditions affect the numerical values of the critical Rayleigh number and the cell dimensions but not the basic validity of the Rayleigh theory (see table 1). In the case of

cloudbands in the free atmosphere, Rayleigh's boundary conditions are actually not unrealistic, while in the convective ground layer a fixed surface at the bottom and an interface at the top would be more appropriate. Jeffrey's critical Rayleigh number (1100) valid for a fixed surface at the bottom and a free upper surface comes closer to this requirement than Rayleigh's (650) but these differences are insignificant in comparison with the magnitude and variation of actual Rayleigh numbers in the atmosphere.

This brings us to a phenomenon which has puzzled many meteorologists: Cellular (Bernard type) cumulus convection is a rather rare event in the atmosphere, except in shallow layers; on the other side, cloudstreets (a special type of cellular convection) are widespread and common. This appears to be the result of the following circumstances:

Due to the depth of the convection layer which enters the Rayleigh number in the 4th power, see (19), the atmospheric Rayleigh numbers are highly supercritical, namely of the order of 10^5 or 10^6 even in the presence of high eddy viscosity and conductivity. As a consequence, normal thermal convection in the atmosphere is turbulent and unsteady (Malkus, 1954) and is strongly affected by thermal inhomogeneties of the ground. Individual convection currents (thermals) rather than an organized cellular convection are the rule in the convective ground layer. In the presence of moderate windshear gradients, however, the Rayleigh number is reduced by many orders of magnitude bringing it close to or even below the critical value. The reason can be seen from (27).

In the atmosphere, the buoyancy term and the vorticity term (in the bracket) are frequently of the same order of magnitude, each being very large in comparison with the viscosity/conductivity term. Only the small difference between these two large quantities is balanced by the third term[7] and in many cases the third term is even larger than this difference suppressing convection all together. By changing the convection pattern to longitudinal bands, nature can eliminate the vorticity term leaving the large buoyancy term unbalanced by the small viscosity/conductivity term. This raises the Rayleigh number (and the growth rate) back to the high values usually found in the atmosphere. Now, however, convection is well organized, in spite of the high Rayleigh number, and while the convective motion is not turbulent in the sense of an unsteady random motion, the presence of strong turbulence within this organized convective structure has been confirmed by glider pilots. (Part I)

This situation is illustrated by figure 5 which shows the influence of the wind shear gradient $\overline{\overline{u}}''$ on the Rayleigh number as a function of the potential temperature gradient θ'. A layer height H of 2 km and an eddy viscosity ν of 10^5 $cm^2\ sec^{-1}$ were assumed. It can be seen that along a diagonal line from the lower left to the upper right the Rayleigh numbers are tightly packed and extremely sensitive to variations in the vertical shear gradient. A change of $\overline{\overline{u}}''$ by one order of magnitude (for example, from 3×10^{-8} to 3×10^{-7} cm^{-1} sec^{-1}, i. e., from 3 m/sec per km^2 to 30 m/sec per km^2) lowers the Rayleigh number from high positive to high negative values (namely from plus 5×10^5 to minus 5×10^6) provided the convection is symmetrical (l = m) and the vertical temperature gradient is close to adiabatic (e. g., $\theta' \sim -0{,}1$°/km). The high negative Rayleigh number will completely suppress symmetrical convection whereas for l = 0 the Rayleigh number will stay at its high positive value and cause vigorous convection in longitudinal bands.

It should be mentioned at this point that very little is known about the average temperature gradient of a convective atmospheric layer. Vertical temperature soundings are accurate only to about ½ degree. It is generally assumed that deviations from the adiabatic temperature gradient in dry air are small. It is unlikely, however, that the adiabatic state is approximated to better than 1/10°/km since temperature differences connected with thermals are of the order of one degree. Figure 5 shows that a mean θ' of –1/1000° C per km is sufficient to exceed the critical Rayleigh number (19) and initiate convection. Therefore, it appears plausible that the atmospheric Rayleigh numbers are highly supercritical.

In cases of condensation, the mechanism of entrainment has the following effect: The widening of the cone of rising air with height dilutes the water content of the cloud. As a consequence, the convection cell is deformed and cloud evaporation in its descending portion occurs at a higher level than condensation at the cloud base creating large dry areas between clouds. In this way, the average vertical temperature gradients inside the convective cloud and in the surrounding clear areas differ with regard to their respective adiabatic stratifications. Vertical soundings taken in these clear areas under cumulus conditions show that temperature gradients at levels above cloudbase are stable with regard to the dry adiabates and unstable with regard to the moist adiabates, the implication being that an atmospheric convection cell with cloud formation is poorly described by an *average* potential temperature gradient θ'. The motion may well be amplified inside the cloud and damped outside.

This in turn must affect the diffusivities such that their values in the horizontal and vertical plane (i. e., along and across potential temperature planes) may be quite different. Some consequences of this particular situation will be discussed below in connection with the observation of giant convection cells.

In a strict sense, the above theory therefore cannot cover the complications introduced by the condensation process in atmospheric clouds while it may well apply to convection in dry air. The actual flow differences between the two types of convection in the atmosphere are not well known at this time.

Fig. 5

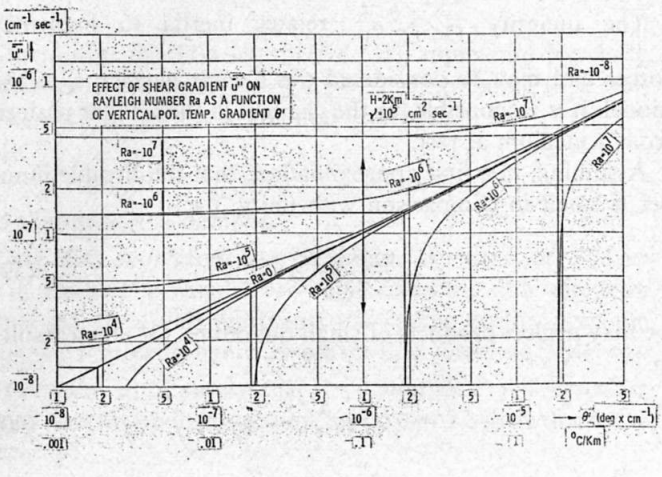

[7] This balance is the meaning of the critical Rayleigh number.

Figure 6 illustrates the shear gradient $\overline{\overline{u}}''$ required to reduce the buoyancy term to zero as a function of the height H of the convective layer. The interdependence of $\overline{\overline{u}}''$ and H follows from (27), (17), and (18), setting the bracket in (27) to zero. Assumed is symmetrical convection with optimum cell dimensions and a plausible range of vertical gradients θ', see (43). The lines from the lower right to the upper left depict the conditions under which the vorticity forces (resulting from the curvature $\overline{\overline{u}}''$ of the wind profile) cancel the buoyancy forces (resulting from the potential temperature gradients θ'). Also plotted are those cloudband observations in Part I and II, where both layer height and shear gradients are known. This figure confirms the highly suppressive effect of the observed wind profiles on normal symmetric convection cells.

If there are large areas of clear air between convective clouds and if the stratification above cloud base is unstable inside the cloud but stable outside, the "Austausch" in the large clear areas will occur primarily along the horizontal planes of potential temperature. As a consequence, the eddy viscosity may be much larger in the horizontal direction (x, y) than in the vertical direction (z). Introducing this case into our equations $\left(\nu^*_{x,\,y} \geqslant \nu^*_z\right)$ the cell dimensions are changed in the fashion indicated by Table 1. If, for example, $\nu^*_{x,\,y} = 10^{>}$ and $\nu^*_z = 10^5$ cm² sec^{-1} the horizontal cell dimension D would be about 20 to 30 times the vertical dimension H. In the atmosphere this calls for cells of 20 to 50 miles diameter. The fact that the upcurrents (clouds) are located along the cell rims indicates a sense of circulation which truly corresponds to the behavior of cellular convection in a gas. (In contrast, the opposite sense of circulation in isolated thermals or cumulus clouds raises questions about the nature of normal atmospheric convection.)

Applying Table 1 and the above reasoning to two dimensional cells, the wide spacing of cloudbands occasionally observed in the atmosphere may find a plausible explanation.

Finally, attention is called to a photogrametric investigation of *cirrus bands* by Reuss (1964 a, b) which indicates that these bands line up with the "thermal jetstream", i. e., with the isotherms at their level. These are frequently but not always parallel to the absolute wind vector. Since the thermal wind direction identifies the wind shear vector and

Fig. 6

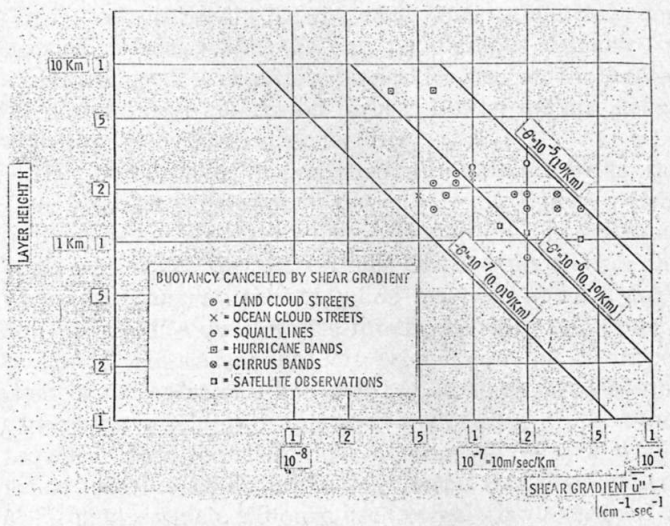

Boundaries		Rayleigh Nr.	D/H Square	D/H Bands	D/H Hexagon (inner)
free, free	$\nu_{x,\,y} = \nu_z$	658	4.0	2.83	3.28
	$\nu_{x,\,y} \gg \nu_z$	658	$2.83\left(\frac{\nu_x \nu_y}{\nu_z}\right)^{1/2}$	$2.0\left(\frac{\nu_x \nu_y}{\nu_z}\right)^{1/2}$	
free, fixed		1,100	3.28	2.34	2.7
fixed, fixed		1,708	2.8	2.0	2.32

Table 1

cirrus bands are found to develop in layers of vertically changing shear, it appears that this high level cloud type obeys similar laws as convection bands near the ground, the measured shear gradients being again of the typical magnitude (10^{-7} cm^{-1}sec^{-1}). Reuss' findings are of special interest to the problem of high level and clear air turbulence near jet streams where circulations of this type may develop with or without cloud formation.

C. Conclusions and Application for Soaring Flight

The theory presented in the foregoing section suggests that cloudstreets form in moving air when the wind profile is sufficiently curved to create vorticity forces which are of comparable magnitude as the buoyancy forces in symmetrical convection. The typical meteorological situation for this condition is given when strong advection of cold air occurs over warm ground or water. In this case, the geostropic wind decreases upwards and the wind direction stays uniform throughout the friction layer.

The sailplane pilot can utilize these predictable weather situations which occur primarily in the spring. The proper soaring technique is straight flight at the cloud base. There is little use entering the cloud as the wind may decrease at higher levels. Weather satellite pictures can help to identify favorable conditions. Prediction and aerological identification from pibals is possible. Systematic utilization of cloudstreet conditions will allow flights in excess of 1,000 km.

References:

(1) *J Kuettner (1959):* "The Band Structure of the Atmosphere", TELLUS *II*, 267 (Part I).

(2) *Alaka, Queney, et al. (1960):* "The Air Flow over Mountains", World Meteorological Organization, Tech. Note No. 34, Geneva.

(3) *H. Jeffreys (1926):* "The Stability of a Layer of Fluid Heated Below", Phil. Mag. *2*, 833.

(4) *C. C. Lin (1955):* "The Theory of Hydrodynamic Stability", Cambridge.

(5) *J. Lumley and H. Panofsky (1964):* "The Structure of Atmospheric Turbulence", John Wiley & Sons, New York.

(6) *W. V. R. Malkus (1954):* "Discrete Transitions in Turbulent Convection", Proc. Roy. Soc., A 225, p. 196.

(7) *A. Pellew and R. Southwell (1940):* "On Maintained Convective Motion in a Fluid Heated from Below", Proc. Roy. Soc., A 176, 312.

(8) *Lord Rayleigh (1916):* "On Convection Currents in a Horizontal Layer of Fluid When the Higher Temperature is on the Under Side", Phil. Mag. 32, 529.

(9) *J. Reuss (1964a):* "Cirren in vertikaler Windscherung", Beiträge zur Physik der Atmosphäre, *36*, 173.

(10) *J. Reuss (1964b):* "The Geometry of Cirrus Bands as Related to Meteorological Conditions", Final Scientific Report, Contract AF 61 (052)–620, July 1964.